Soft Matter

Accepted Manuscript

Volume 1 | Number 1 | Jan 2013 | Pages 1–100

Soft Matter

www.rsc.org/softmatter

ROYAL SOCIETY OF CHEMISTRY

ROYAL SOCIETY
OF **CHEMISTRY**

www.rsc.org/softmatter

Soft Matter

Selective and visual Ca^{2+} ion recognition in solution and in a self-assembly organogel of terpyridine-based derivative triggered by ultrasound

Received 00th January 20xx,
Accepted 00th January 20xx

DOI: 10.1039/x0xx00000x

www.rsc.org/

Lijun Geng,‡ Yajuan Li,‡ Zengyao Wang, Yanqiu Wang, Guoliang Feng, Xuelei Pang, Xudong Yu*

Abstract: a new kind of terpyridine-based Ca^{2+} sensor **TS** based on internal charge transfer (ICT) was designed and studied. In the diluted solution state, **TS** sensed Ca^{2+} and Mg^{2+} ions among test ions via "off–on" approach as seen from fluorescence spectra among test ions. Moreover, **TS** was able to form stable fluorescent gels in organic solvents accelerated by ultrasound, indicating the ultrasound responsive properties of **TS** molecules. The S-gel of **TS** could be successfully used to selectively recognize Ca^{2+} through fluorescent emission color and morphological changes, which was different from that of the solution state. It was predicated that the competition between the self-assembly of **TS** molecules and host-guest interaction of **TS** with Ca^{2+} or Mg^{2+} was responsible for the sensing properties. To the best of our knowledge, this is the first example that orgnoagels could selectively sense Ca^{2+} ion.

Introduction

In the past decades, considerable effort has been dedicated to develop fluorescent receptor probes in order to sense biologically important ions.[1-4] Calcium ion plays the vital role in various cellular processes such as intracellular signal messenger, cell death, as well as fluid secretion. Selective and quantitative detection of Ca^{2+} is extremely important to determine their spatial concentration for clarifying their functions in biological systems.[5-8] Considering its importance, several works have been conducted to develop Ca^{2+} probes via fluorescent technique. These probes are usually comprised of dye groups and receptor binding sites such as C=O, COOH as well as crown ether groups. However, very few receptors containing N sites that could selectively bind with Ca^{2+} have been reported. Terpyridine segments are ideal building blocks to coordinate with ions such as Zn^{2+}, Fe^{2+}, Pb^{2+}, Cr^{3+}, Eu^{3+} and Ru^{2+}.[9-16] By proper design, terpyridine derivatives show outstanding properties in the field of sensing, light emitting materials and functional polymer networks. Therefore, construction of terpyridine-based functional systems with Ca^{2+} is of urgency and great importance in the field of biology and functional material science.

Low Molecular Weight Gelators (LMWGs) especially stimulus responsive gels have attracted increasing interest in the past decades.[17-25] In recent years, such responsive gels are extensively developed to create sensing systems toward analytes such as fluoride ion, gas, chiral compounds, as well as pH.[21-31] They often display instant and visual changes to analytes for detection purpose. In our previous works, we reported a series of sonogels (sonication triggered organogels) and studied their gelation mechanisms[18]. Recently, to explore their application in sensing systems, we reported a new kind of sonogel based on cholesterol derivative for instant, reversible and visual recognition of amines.[32] We also developed a lysine-based organogel which exhibited thixotropic properties.[33] Various paradigms of gelators containing the terpyridine group were present in the literature. For example, K. Rissanen studied the hydrogelation behaviour of terpyridine derivatives based on metal ions;[34-35] L. Sambri reported a class of terpyridine based hydrogels accelerated by ultrasound.[36] In the present study, as a continuation of our efforts in developing stimulus responsive gels for sensing purpose, we incorporated 4-amino-terpyridine group with ICT process from N as electron donor and pyridine group as electron acceptor into lysine based gel molecule to generalize a novel fluorescent gelator (**TS**, Scheme 1), which displayed ultrasound responsive property and high selectivity for Ca^{2+} among test ions both in solution and in gel state. Interestingly, the diluted solution of **TS** expressed fluorescent enhancement toward Ca^{2+} or Mg^{2+} ion by "off-on" approach; By contrast, **TS** showed obvious emission color changes from blue to yellow toward Ca^{2+} for visual detection whilst in the gel state (Figure 1). Therefore, the S-gel was selectively responsive to Ca^{2+} compared with Mg^{2+}. Several experiments revealed that the competition between **TS** self-assembly and the interaction of **TS** with ions played the key role for the highly selective sensing of **TS** toward Ca^{2+}.

Hebei Research Center of Pharmaceutical and Chemical Engineering, and College of Science, Hebei University of Science and Technology, Yuhua Road 70, Shijiazhuang 050080, PR China.
E-mail for corresponding author: 081022009@fudan.edu.cn (X. Yu).
‡ Joint first authors contributed equally to this work.
† Electronic supplementary information (ESI) available. See DOI:

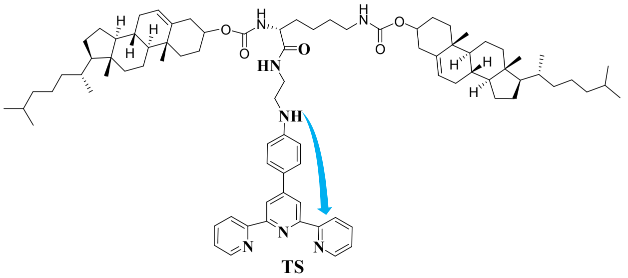

Scheme 1 The chemical structure of **TS** with ICT process.ition and the sol obtained by heating-cooling process in light and in dark (irradiated by 365 nm).

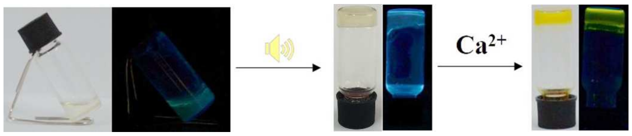

Fig. 1 illustration of ultrasound-accelerated gelation of **TS** for visual sensing of Ca^{2+}.

Experimental

Materials

All starting materials were obtained from commercial supplies and used without further purification. Cholesteryl chloroformate (99%) was obtained from Sigma-Aldrich. Methyl L-lysinate dihydrochloride, 4-Bromobenzaldehyde, 2-Acetylpyridine, HOBt (NHydroxybenzotrizole, 98%), EDC·HCl (1-ethyl-3-(3-dimethyllaminopropyl carbodiie hydrochlide, 98%) and other reagents were supplied from Shanghai Darui fine chemical Co. Ltd.

Techniques

FTIR spectra were recorded by using an IRPRESTIGE-21 spectrometer (Shimadzu). SEM images of the xerogels were obtained by using SSX-550 (Shimadzu) and FE-SEM S-4800 (Hitachi) instruments. Samples were prepared by spinning the gels on glass slides and coating them with Au. NMR spectra were performed on a Bruker Advance DRX 400 spectrometer operating at 500/400 and 125/100 MHz for ^{1}HNMR and ^{13}CNMR spectroscopy, respectively. The high-resolution mass spectra (HR-MS) were measured on a Bruker Micro TOF II 10257 instrument. Fluorescence spectra were collected on an Edinburgh instrument FLS-920 spectrometer with a Xe lamp as an excitation source. The X-ray diffraction pattern (XRD) was generated by using a Bruker AXS D8 instrument (Cu target; λ = 0.1542 nm) with a power of 40 kV and 50 mA. UV-Vis absorption and fluorescent spectra were recorded on a UV-vis 2550 spectroscope (Shimadzu). Sonication treatment of a sol was performed in a KQ-500DB ultrasonic cleaner (maximum power, 100 W, 40 KHz, Kunshan Ultrasound Instrument Co, Ltd., China).

The ion sensing experiments

Nitrite salts of metal ions (Mg^{2+}, Ca^{2+}, Na^{+}, Bi^{3+}, Al^{3+}, Pb^{2+}, Hg^{2+}, Ba^{2+}) and chloride salts of metal ions (Sn^{2+}, Mg^{2+}) were used to evaluate the metal ion binding properties by the synthesized compound **TS**.

Rheology

Rheological measurements were carried out on freshly prepared gels using a controlled stress rheometer (Malvern Bohlin GeminiHRnano). Cone and plate geometry of 40 mm diameter was employed throughout the dynamic oscillatory work.

Results and discussion

The synthesis and characterization of **TS** could be seen from ESI. From an overall consideration of solubility and suitable gelation solvents of **TS** and ions, the ion recognition properties were evaluated in ethyl acetate. We tested the fluorescent sensing activity of **TS** for various ions, e. g. Ca^{2+}, Mg^{2+}, Hg^{2+}, Zn^{2+}, Sn^{2+}, Pb^{2+}, Ni^{2+}, Bi^{3+}, Na^{+}, and Al^{3+}. As seen from Figure 2a and 2b, **TS** displayed obvious “off-on” fluorescent enhancement toward Ca^{2+} and Mg^{2+}, whereas other ions caused fluorescent quenching of **TS**. Similar ions such as Sr^{2+} and Ba^{2+} also triggered little changes of the fluorescent spectra of TS (Fig. S1).

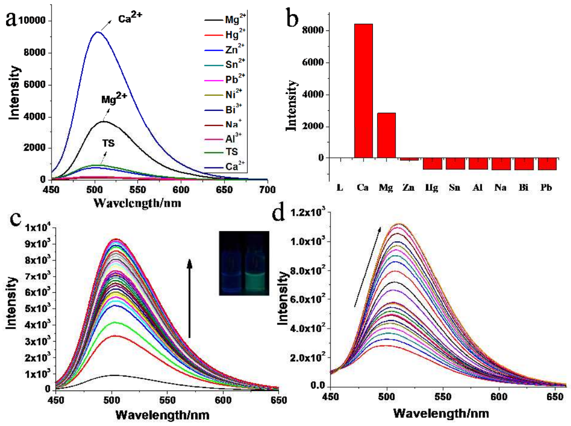

Fig. 2 a) Fluorescence emission spectrum changes of **TS** (10^{-5} M) upon the addition of different ions (50 eq.); b) the intensity changes of **TS** with ions at 502 nm, the value of intensity was calculated by I-I_0; c) fluorescent titrations of **TS** with Ca^{2}+; d) fluorescent titrations of **TS** with Mg^{2+}.

To further illustrate the quantitative sensing of **TS** (10^{-5} M) toward Ca^{2+} or Mg^{2+}, fluorescent titrations were carried out. As shown in Fig. 2c, the intensity of the fluorescent peak of **TS** at 502 nm was remarkably increased by 10.1 fold upon the addition of Ca^{2+} ions (0-20 eq). By contrast, the addition of Mg^{2+} (0-6 eq.) triggered 8 nm red shift of **TS** solution from 502 nm to 510 nm, together with fluorescent enhancement by 4 fold (λ_{em}=502 nm). The results revealed the different binding ability of Ca^{2+} and Mg^{2+}. By plotting the fluorescent intensity changes of **TS** at 502 nm, as a function of 1/[ion] (1/[I-I_0] vs

1/[ion]), a linear curve was observed that changed over two units, which was characteristic of a 1:1 binding mode. The binding constant of **TS** with Ca^{2+} and Mg^{2+} was determined to be $5.3\times10^{5}M^{-1}$ and $3.44\times10^{3}M^{-1}$ respectively (Fig. S2, S3), and the detection limit was 1.93×10^{-8} and 1.30×10^{-5} M (ESI). The above results suggested that when **TS** was bonded with Ca^{2+} or Mg^{2+}, the charge of the terpyridine group was transferred to the cation. Thus, the electron transfer from the amine electron donor to terpyridine group became more favourable and finally caused fluorescence enhancement.

In the presence of mixed ions including Ba^{2+}, Sr^{2+} and Mg^{2+} ions (50 eq.), Ca^{2+} ion triggered the fluorescent intensity enhancement of **TS** by a factor of 9.5. While, in the presence of all the tested ions, the fluorescence intensity of **TS** increased by 5.6 fold (Fig. S4). The above results revealed that **TS** had high selectivity for Ca^{2+} via “off-on” approach even in the condition of mixed ions.

The gelation ability by the self-assembly of **TS** via intermolecular interaction was evaluated in organic solvents using a test tube inversion method. By the classic heating-cooling process, no gel formed in the test solvents. Amazingly, brief irradiation of **TS** solution (25 mg/mL) in ethyl acetate turned the homogenous solution into a stable opaque gel. Gelation accelerated by sonication was also observed in the solvents of benzene, acetone, glycol monomethyl ether, and cyclohexane, indicating the exclusively sonication responsive properties of **TS** molecule or assembly (Table 1). The switchable sol-gel/precipitate-gel transitions could be repeated without fatigue by heat and sonication stimuli.

The stiffness is an important factor for constructing organogels and hydrogels.[36] The rheological properties of **TS** in ethyl acetate was measured (Fig. 3). It could be seen that the value of the viscosity decreased with the increasing sweep frequency (from 0 to 100 rad/s), indicating the shear thinning property. Keeping strain at 1%, the elastic storage modulus (G′) was much greater than the loss modulus (G′′), this meant a good gel state. Also, G′ and G′′ were in the linear viscoelastic region (LVR). The above results indicated that **TS** in ethyl acetate possessed good mechanical property.

As a typical example, the spectroscopic and microscopy studies were performed in ethyl acetate. **TS** solution (10^{-5} M) showed two peaks at 288 and 335 nm, which was ascribed to the ICT process of the terpyridine segment. The UV-vis spectra of the S-gel banded at 390, 437 nm displayed 102 nm red shift from the solution, indicating the J aggregate of terpyridine unit in gel state (Fig. 4a). From Fig. 4b, the fluorescent band of S-gel at 509 nm was 8 nm red-shifted compared to that of solution at 501 nm, suggesting π-π interactions of **TS** molecules in the gel tissue. However, the powder obtained from column and S-xerogel had very similar IR spectra, both displayed –NH vibrations at 3442 cm^{-1} and C=O vibrations at 1638 cm^{-1} as seen from Fig. 4c.

Fig. 5 displayed the gradually fluorescent color changes of **TS** gel after the addition of Ca^{2+} ion (5 eq.). After aging for 4 hours, Ca^{2+} ion completely penetrated into the gel network, and the emission color of the gel changed from blue to yellow (irradiated at 365 nm, Fig. 5). On the contrary, the contact site of the S-gel with Mg^{2+} only displayed fluorescent off phenomena, and Mg^{2+} did not penetrated in to the gel networks even after 24 hours (different kinds of Mg^{2+} salts such as $Mg(NO_3)_3$, $MgCl_2$ and $MgSO_4$ were used).

Table 1 the gelation properties of **TS** (25 mg/mL)

Solvent	H-C	S
1,4-dioxane	P	S
n-propanol	S	S
methanol	S	S
ethanol	P	P
butanol	S	S
ethyl acetate	S	OG
acetone	P	OG
THF	S	S
chloroform	S	S
glycol monomethyl ehter	P	OG
benzene	S	OG
n-hexane	S	S
acetonitrile	P	P
cyclohexane	P	TG

Note: P: precipitate; S: solution; OG: opaque gel; TG: transparent gel.

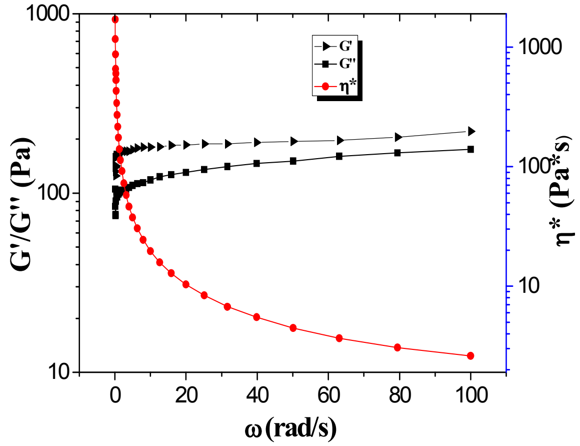

Fig. 3 Dynamic frequency sweep data of gel **TS** in ethyl acetate and plots of η* as function of ω; c) evolution of G', G'' as functions of ω (from 0 to 100 rad/s, strain: 1%).

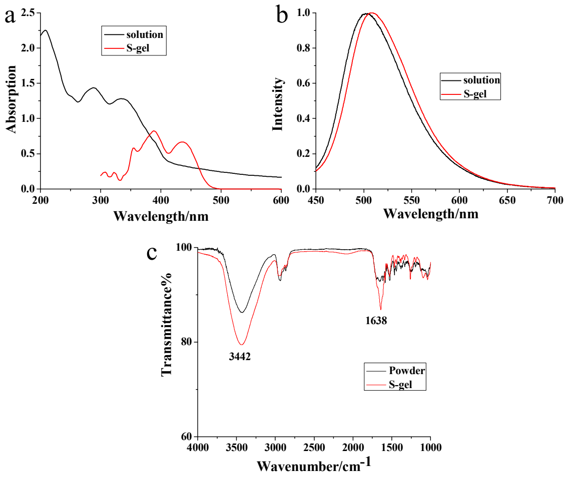

Fig. 4 a) Uv-vis spectra of solution (10^{-5} M) and gel of **TS** (25mg/mL), the solution was tested using a quartz cell, and gel was tested using a quartz film; b) the fluorescence spectra of solution (10^{-5} M) and gel of **TS** (25mg/mL); c) the FT-IR spectra of powder from evaporation and S-gel (25 mg/mL) of **TS**.

Fluorescence spectra was used to monitor the fluorescent changes of S-gel and S-gel with Ca^{2+}. The maximum fluorescence emission of S-gel with Ca^{2+} showed 46 nm red shift compared with that of S-gel at 509 nm, together with fluorescence quenching by 1.1 fold (Fig. 6). The result was in accordance with the emission color changes. Upon heating the gel with Ca^{2+} (10 eq.) from 25 °C to 80 °C with a gel-to-suspension transformation, the maximum intensity peaks displayed obvious blue shift from 554 nm to 516 nm and fluorescence enhancement by a factor of 3.5 (Fig. S5). SEM images was used to track the morphology changes of the direct sol-to-gel then gel-to-gel transition triggered by ultrasound and Ca^{2+} (Fig. 7). The powder obtained from the sol (25 mg/mL) by evaporation method was comprised of irregular sheet structure, which was transformed into porous membrane structure in S-gel state (with pore diameters ranging from 20 nm to 1 μm). After binding of TS assembly with Ca^{2+} in the gel tissue, fibrous networks in nano scale were observed, which indicated that Ca^{2+} ions were inserted into the gel networks through coordination interaction. The UV-vis spectra were also performed to examine the aggregate changes of TS assembly. Seen from Fig. S6, two groups of peaks banded at 291 and 324 nm, 376 and 398 nm appeared, which were rationally ascribed to the absorption peaks of **TS** assembly with Ca^{2+} ion. The result also suggested that the π-π stacking mode of terpyridine segment was changed by the addition of Ca^{2+} although the gel maintained its state.

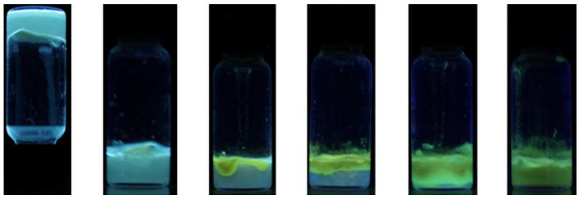

Fig. 5 photos of **TS** gel after coated with Ca^{2+} (in dark irradiated by 365 nm), from left to right: S-gel of **TS**; addition with Ca^{2+} immediately; after 30 min; after 1 h; after 2 h; after 3 h.

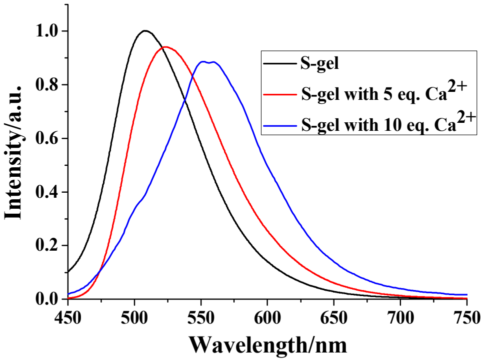

Fig. 6 Normalized fluorescence spectra of S-gel and S-gel with Ca^{2+} (5 eq., and 10 eq.), the fluorescence spectra were tested *in situ* using the same cell.

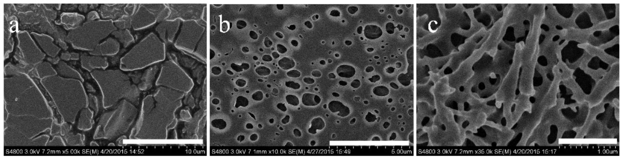

Fig. 7 SEM images of **TS** assembly; a) powder of **TS** assembly from evaporation (25 mg/mL); b) S-gel of **TS** assembly (25 mg/mL); c) S-gel of **TS** assembly (25 mg/mL) with Ca^{2+} (5 eq.). Scale bar: 10 μm, 5 μm, 1 μm.

From the above results, the sensing properties of **TS** toward ions could be summarized as following: In the solution state, the binding of Ca^{2+} or Mg^{2+} with **TS** facilitated the ICT process of the terpyridine segment, resulting in the fluorescence enhancement. When triggered by sonication, **TS** captured solvent to form a gel with porous membrane structure, through the J aggregate of terpyridine groups, hydrogen bonding as well as hydrophobic interactions.

The self-assembly force of **TS** molecules was stronger than that of **TS** with Mg^{2+}, and weaker that of **TS** with Ca^{2+}. Therefore, Ca^{2+} ions were able to penetrate into the gel network through coordination interaction and partially changed the π-π stacking mode of terpyridine groups, thus resulting in the microscopic changes of **TS** gel, including emission color and morphology changes. Such changes would allow the gel to behave as visual and selective sensor toward Ca^{2+}.

Conclusions

In summary, a new kind of terpyridine based orgnaogel accelerated by sonication was designed and characterized. The gel exhibited outstanding sensing properties toward Ca^{2+} ion, exhibiting obvious emission color and morphology changes in the presence of Ca^{2+}. On the other hand, in the solution state, **TS** could be served as an efficient "off-on" sensor for Ca^{2+} or Mg^{2+}. It was proposed that the competition between the host-host interaction and the host-ion interaction were responsible for recognition events. To the best of our knowledge, this is the first report of modification of ICT processes in a terpyridine-based compound by ions in either solution or gel state, which provided a new method for constructing ion sensors.

Acknowledgements

The authors thanks for the financial support by NNSFC (21401040, 21301047), Xiaoli fund SW(2014PT91), Youth Foundation of Hebei Province Department of Education Fund (QN2014127), Natural Science Foundation of Hebei Province (No.B2014208160, B2014208091).

Notes and references

1 M. C.-L. Yeung and V. W.-W. Yam, *Chem. Soc. Rev.,* 2015, **44**, 4192-4202.
2 P. A. Gale, *Chem. Soc. Rev.,* 2010, **39**, 3746-3771.
3 Y. Zhou, J. F. Zhang and J. Y. Yoon, *Chem. Rev.,* 2014, **114**, 5511-5571.
4 Q. Zhao, F. Li and C. Huang, *Chem. Soc. Rev.,* 2010, **39**, 3007-3030.
5 X. Dong, Y. Yang, J. Sun, Z. Liu and B. Liu, *Chem. Commun.,* 2009**,** 3883–3885.
6 H. Komatsu, T. Miki, D. Citterio, T. Kubota, Y. Shindo, Y. Kitamura, K. Oka and K. Suzuki, *J. Am. Chem. Soc.*, 2005, **127**, 10798-10799.
7 E. Carafoli, *Proc. Natl. Acad. Sci. U.S.A.***,** 2002, **99**, 1115-1122.
8 S. Watanabe, S. Ikishima, T. Matsuo and K. Yoshida, *J. Am. Chem. Soc.,* 2001, **123**, 8402-8403.
9 D. Y. Wang, H. F. Wang and H. R. Li, *ACS Appl. Mater. Interfaces,* 2013, **5**, 6268–6275.
10 M. R. Dewi, T. A. Gschneidtner, S. Elmas, M. Ranford, M.-P. Kasper and T. Nann, *ACS Nano,* 2015, **9**, 1434-1439.
11 X. C. Lu, X. P. Li, K. Guo, T. Z. Xie, C. N. Moorefield, C. Wesdemiotis and G. R. Newkome, *J. Am. Chem. Soc.*, 2014, **136**, 18149–18155.
12 A. Wild, A. Winter, F. Schlütter and U. S. Schubert, *Chem. Soc. Rev.,* 2011, **40**, 1459-1511.
13 Y. Ding, P. Wang, Y. K. Tian, Y. J. Tian and F. Wang, *Chem. Commun.,* 2013, **49**, 5951-5953.
14 R. Wang, M. Geven, P. J. Dijkstra, P. Martens and M. Karperien, *Soft Matter*, 2014, **10**, 7328-7336.
15 Y. Y. Tanaka, K. M.-C. Wong and V. W.-W. Yam, *Chem. Sci.*, 2012, **3**, 1185-1191.
16 X. Z. Li, X. P Zhou, D. Li and Y. G. Yin, *Cryst. Eng. Comm.,* 2011, **13**, 6759-6765.
17 X. D. Yu, P. Zhang, Y. J. Li, L. M. Chen, T. Yi and Z. C. Ma, *Cryst EngComm,* 2015, 10.1039/C5CE00636H.
18 X. D. Yu, L. M. Chen, M. M. Zhang and T, Yi, *Chem. Soc. Rev.,* 2014, **43**, 5346-5371.
19 S. S. Babu, V. K. Praveen and A. Ajayaghosh, *Chem. Rev*., 2014, **114**, 1973−2129.
20 X. D. Yu, Q. Liu, J. C. Wu, M. Zhang, X. Cao, S. Zhang, Q. Wang, L. Chen and T. Yi, *Chem. Eur. J.,* 2010, **16**, 9099-9106.
21 N. Yan, Z. Y. Xu, K. K. Diehn, S. R. Raghavan, Y. Fang and R. G. Weiss, *J. Am. Chem. Soc.*, 2013, **135**, 8989–8999.
22 X. H. Cao, L. Y. Meng, Z. H. Li, Y, Y. Mao, H. C. Lan , L. M. Chem, Y. Fan and T. Yi, *Langmuir,* 2014, **30**, 11753−11760.
23 Y. Zhang , H. Ding , Y. F. Wu , C. X. Zhang , B. L. Bai , H. T. Wang and M. Li, *Soft Matter,* 2014*,* **10**, 8838-8845
24 P. C. Xue, B. Q. Yao, J. B. Sun, Z. Q. Zhang and R. Lu, *Chem. Commun.,* 2014, **50**, 10284-10286.
25 B. Adhikari, C. Singh, A. Shah, A. J. Lough and H. B. Kraatz, *Chem. Eur. J.*, 2015, DOI: 10.1002/chem.201501395.
26 X. Zhang, S. Y. Lee, Y. F. Liu, M. J. Lee, J. Yin, J. L. Sessler and J. Y. Yoon, *Scientific Reports*, 2014, **4**, 4593.
27 T. Tu, W. Fang, X. Bao, X. Li and K. H. DÖtz, *Angew. Chem. Int. Ed*., 2011, **50**, 6601–6605.
28 G. O., Lloyd and J. W., Steed, *Nat. Chem.,* 2009*,* **1**, 437-442.
29 Y.Gao, J. Shi, D. Yuan and B. Xu, *Nat. Commun.*, 2012, **3**, 1033.
30 S. Sarkar, S. Dutta, S. Chakrabarti, P. Bairi and T. Pal, *ACS Appl. Mater. Interfaces*, 2014, **6**, 6308-6316.
31 S. C. Wei, M. Pan , K. Li , S. J. Wang, J. Y. Zhang and C. Y. Su, *Adv. Mater.*, 2014, **26,** 2072-2077.
32 X. L. Pang, X. D. Yu, H. C. Lan, X. T. Ge, Y. J. Li, X. L. Zhen and T. Yi, *ACS Appl. Mater. Interfaces,* 2015, **7**, 13569−13577.
33 X. D. Yu, X. Cao, L. Chen, H. Lan, B. Liu and T. Yi, *Soft Matter,* 2012, **8**, 3329-3334.
34 B. N. Ghosh, S. Bhowmik, P. Mal and K. Rissanen, *Chem. Commun.,* 2014, **50**, 734-736.
35 S. Bhowmik, B. N. Ghosh and K. Rissanen, *Org. Biomol. Chem.,* 2014, **12**, 8836-8839.
36 L. Sambri, F. Cucinotta, G. D. Paoli, S. Stagni and L. D. Cola, *New J. Chem.*, 2010, **34,** 2093-2096.
37 Z. C. Ma, P. Zhang, X. D. Yu, H. C. Lan, Y. J. Li, D. Y. Xie, J. Y. Li and T. Yi, *J. Mater. Chem. B,* 2015, DOI: 10.1039/c5tb01191d.